

Electrochemical Properties of  $\alpha$ -Ferric Oxide in Sulfuric Acid Solutions

Hiroshi YONEYAMA and Hideo TAMURA

*Department of Chemical Technology, Faculty of Engineering, Osaka University, Suita, Osaka*

(Received August 4, 1969)

I-V curves of the  $\alpha$ -Fe<sub>2</sub>O<sub>3</sub> electrode containing different amounts of Ti were obtained potentiostatically in H<sub>2</sub>SO<sub>4</sub> solutions. The anodic current, indicating the dissolution reaction, was almost constant and was not affected by the  $a_{H^+}$  of the electrolyte in the potential range 0.4–1.0V vs. SCE, but it was dependent on the conductivity of the electrode. It was suggested that the dissolution reaction of this electrode is governed by the electron-transfer mechanism, much as is that of the heavily-doped N-type Ge. The flat-band potential of the  $\alpha$ -Fe<sub>2</sub>O<sub>3</sub> electrode was estimated on the basis of the capacity measurement. This potential changed with the  $a_{H^+}$  of the electrolyte.

The mechanism of electric conduction in 3d transition metal oxides<sup>1)</sup> deviating a little from stoichiometry have been considered to be different from that in the usual semiconductors, such as Ge and ZnO. In a previous paper<sup>2)</sup> we studied redox reactions on lithiated NiO showing P-type conduction and made it clear that the electrical property of the electrode determined the electrochemical reactions on it. A study of the electrochemical reactions of N-type 3d transition metal oxide is a useful course of study in elucidating the effect of the electrical property of the electrode on the reactions.  $\alpha$ -Fe<sub>2</sub>O<sub>3</sub> containing Ti is a typical N-type semiconductor among 3d transition metal oxides.<sup>3,4)</sup> Therefore, we planned to study the electrochemical properties of  $\alpha$ -Fe<sub>2</sub>O<sub>3</sub> as a step in the study of the reactions on this electrode. In this paper the polarization behavior and the differential capacity of this electrode will be discussed.

## Experimental

**Electrode.** High-purity Fe power (99.99% up) was dissolved in hot H<sub>2</sub>SO<sub>4</sub> solution, and then the hot solution was filtered. FeSO<sub>4</sub> was precipitated from the filtrate on cooling it. The precipitate was washed by decantation, filtrated, and washed with deionized water and then with CH<sub>3</sub>OH. After having been dried, the FeSO<sub>4</sub> was decomposed to Fe<sub>2</sub>O<sub>3</sub> in the air at 450°C. The Fe<sub>2</sub>O<sub>3</sub> prepared in this way was mixed with 0.2–1.0 atom % Ti in the form of high purity TiO<sub>2</sub> (99.9% up) and ground in an agate mortar. The mixture was pressed into a tablet at 2.25 t/cm<sup>2</sup> (15 mm dia and 3–4 mm thick). This tablet was fired in the air for 4.5 hr at 1200°C and for 5 hr at 1300°C. The tablets shrank to a

diameter of about 10 mm during sintering, though they still had an apparent porosity of about 20%. Platinum contacts on the end faces of the tablet were made by firing platinum powder pasted on them at 1250°C as a contact material for soldering a lead wire. As the electrical lead was needed for mechanical strength, the vapor-deposition technique was not adopted for making the contact on  $\alpha$ -Fe<sub>2</sub>O<sub>3</sub>. The conduction type of the sample was checked by thermo-electromotive force measurements and was found to be of the N-type, as had already been reported by Morin<sup>3)</sup> and by Verway and his co-workers.<sup>4)</sup> This sample was fabricated into a electrode in the same way as was used in the study of the lithiated NiO electrode,<sup>5)</sup> after the apparent resistivity of the sample had been estimated by the voltage-drop method. Silver and indium were also used to make the electrical contact to  $\alpha$ -Fe<sub>2</sub>O<sub>3</sub>. Ag contact was made by firing Ag powder pasted on an end face of the tablet of  $\alpha$ -Fe<sub>2</sub>O<sub>3</sub> at 900°C. Indium contact was made by soldering the indium, though the soldering was often unsuccessful. In the case of indium contact, the contact area was restricted to a part of an end face of the tablet of  $\alpha$ -Fe<sub>2</sub>O<sub>3</sub>, since impregnation of a benzene solution of polystyrene was necessary after mounting a specimen in glass tube. The sample used in this study had the Ti content and contact material shown in Table 1. The electrode area was estimated by the method described previously.<sup>6)</sup> In this estimation the ac resistance measured in 2 N H<sub>2</sub>SO<sub>4</sub> was chosen as the resistance of the electrode. After all the measurements described below, the  $\alpha$ -Fe<sub>2</sub>O<sub>3</sub> specimen was taken out of the glass tube and its surface was erased with emery paper. The specific resistivity of the  $\alpha$ -Fe<sub>2</sub>O<sub>3</sub> used in this study was then estimated by the four-probe method.<sup>6)</sup> This value is shown in Fig. 1 as a function of the Ti content.

**Cell Equipment.** The cell equipment has been described previously.<sup>2)</sup> The counter electrode was a platinized platinum net (2×4 cm). The test electrode was conditioned by pre-electrolysis in 0.1 N H<sub>2</sub>SO<sub>4</sub> at 1.2V and 0.2V vs. SCE each 20–30 min.

**Electrolyte.** 0.1, 0.2, 0.5, and 1.0 N H<sub>2</sub>SO<sub>4</sub> were

1) F. J. Morin, *Bell System Tech. J.* **37**, 1047 (1958).  
2) H. Yoneyama and H. Tamura, *This Bulletin*, to be published.

3) F. J. Morin, *Phys. Rev.* **83**, 1005 (1951), *ibid.*, **93**, 1195 (1954).

4) E. J. W. Verway, P. W. Haaijman and F. C. Romeijn, *Chem. Weekblad*, **44**, 705 (1948).

5) H. Yoneyama and H. Tamura, *This Bulletin*, **42**, 1795 (1969).

6) L. B. Valdes, *Proc. IRE*, **42**, 420 (1954).

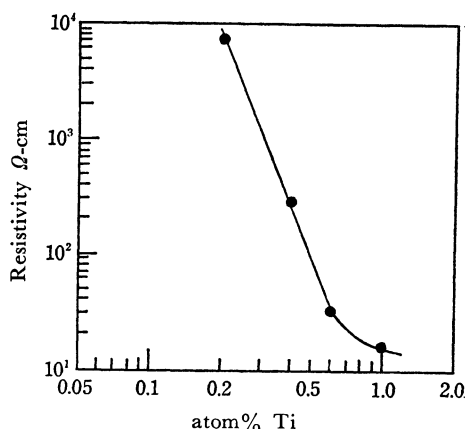


Fig. 1. Resistivity of  $\alpha\text{-Fe}_2\text{O}_3$  as a function of Ti content.

prepared using analytical-grade  $\text{H}_2\text{SO}_4$ .

**Bridge.** The bridge was constructed after the model of Toshima and Uchida.<sup>7)</sup> The arrangement is shown in Fig. 2. The ac input voltage into the bridge circuit was set in 3 mV. 2.5, 5, and 10 kc were chosen as the ac frequencies. The null point was detected by a tuned-null detector with a 70 db gain.

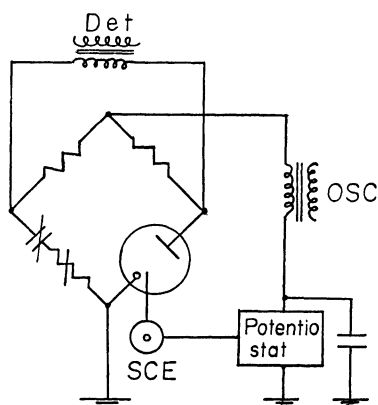


Fig. 2. Bridge arrangement with a potentiostat for superposition of AC with DC voltage.

### Results and Discussion

When the electrode was polarized potentiostatically, the current flow was suppressed in the 0.4–1.0 V potential region. Typical I-V curves are shown in Fig. 3. The current attained a stationary value within 5 min—2 hr<sup>8)</sup> after the potential setting. I-V curves was usually obtained with a potential raising, but if it was done with a potential lowering from 1.5 V the steady-state current was somewhat smaller. The I-V curves can be separated into three regions, as is indicated in Fig. 3. In the

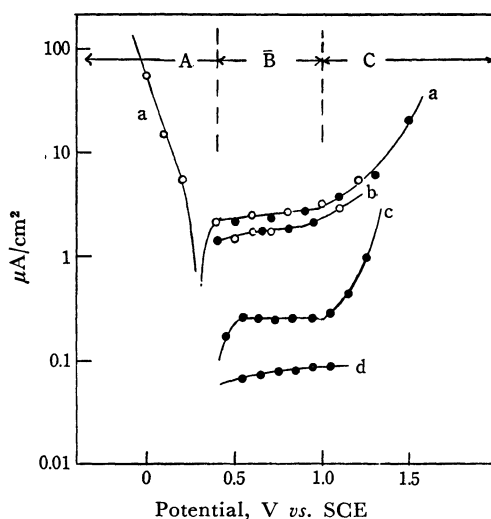


Fig. 3. I-V curves of  $\alpha\text{-Fe}_2\text{O}_3$  in  $\text{H}_2\text{SO}_4$  solutions. Electrode had the following Ti content. (atom%). a; 1.0, b; 0.6, c; 0.4, and d; 0.2 electrolyte: —○— 1 N —●— 0.1 N

region A, the I-V curve refers to the hydrogen evolution reaction or the reduction reaction of the electrode, while oxygen evolution possibly occurs in the region C. In the region B the current was not affected by the stirring of the electrolyte or by the concentration of sulfuric acid, as Fig. 3 shows. According to the potential-pH diagram,<sup>9)</sup>  $\text{Fe}_2\text{O}_3$  is not stable in the region B. In order to clarify the nature of the current in the region B, the quantity of Fe dissolved into the electrolyte after the electrode C had been polarized potentiostatically at 0.9 V for a known period and then compared with the quantity of electricity passed through during the polarization. As a result, 16  $\mu\text{A}\cdot\text{H}$  produced 32.5  $\mu\text{g}$  Fe; i.e., one faraday amounts to 54.5 g Fe. From this result, the current in the region B can be said to refer to the anodic dissolution reaction of the electrode.

When a N-type semiconductor comes in contact with a metal having a large work function, a potential barrier is formed on the contact face depending on the difference between their work functions, and then a space-charge layer is created in the interface. As platinum has a large work function, 5.10 eV,<sup>10)</sup> a potential barrier should have been formed on the interface between Pt and  $\alpha\text{-Fe}_2\text{O}_3$ . Such a potential barrier occasionally controls the current flow. However, the Pt- $\alpha\text{-Fe}_2\text{O}_3$  contact did not control the electrochemical reactions even if the potential barrier existed at the contact face, for generally a current flow is hindered cathodically by this barrier

7) S. Toshima and I. Uchida, *Denki Kagaku*, **34**, 624 (1966).

8) Nearly 2 hr was required at 0.5 V with the potential raising measurement.

9) M. Pourbaix, "Atlas of the Electrochemical Equilibria in Aqueous Solution," Pergamon Press, Oxford, London (1966), p. 307.

10) "Landolt-Börnstein," 6 Aufl., Bd./6, Springer-Verlag, Berlin, Gottingen, Heidelberg (1959), p. 913.

if the electrochemical reactions are controlled by this barrier, but a distinct current appeared in the region A. Moreover, a distinct cathodic current showing the reduction of  $\text{Fe}^{3+}$  was observed in the potential comparable to the region B.<sup>11)</sup> The suppression of the anodic current flow in the region B does not, therefore, stem from Pt- $\alpha\text{-Fe}_2\text{O}_3$  contact.

In the anodic dissolution reaction of the common semiconductors, a saturation current is usually observed in N-type semiconductors.<sup>12-14)</sup> The holes are connected with this current flow. As a hole probably exists in  $\alpha\text{-Fe}_2\text{O}_3$ ,<sup>15)</sup> hole-connected mechanism cannot be simply denied. In order to clarify this point, an I-V curve was obtained in the electrolyte containing  $\text{Ce}^{4+}$ . If hole is connected with the anodic dissolution reaction, the current should increase in the electrolyte containing  $\text{Ce}^{4+}$  compared with the case when only  $\text{H}_2\text{SO}_4$  is present because the holes injected from the reduction of  $\text{Ce}^{4+}$  would participate in the dissolution reaction.<sup>16)</sup> Of course, this method may not be complete for determining the kind of charge carrier involved in the reaction, since some particular effects, such as the Hall effect and carrier injection, which can be observed in common semiconductors have not been observed in 3d transition metal oxides.<sup>1)</sup> The I-V curves obtained in each electrolyte are shown

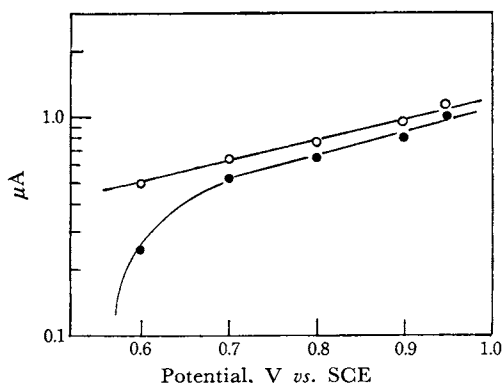


Fig. 4. I-V curves of  $\alpha\text{-Fe}_2\text{O}_3$  in the electrolyte of —○— 1 N  $\text{H}_2\text{SO}_4$  and —●— 0.01 M  $\text{Ce}^{4+}$ /1 N  $\text{H}_2\text{SO}_4$ . Measurement was carried out with potential decreasing direction at the B electrode.

11) H. Yoneyama, S. Hamamatsu and H. Tamura, *This Bulletin*, to be published.

12) D. R. Turner, *J. Electrochem. Soc.*, **103**, 252 (1956).

13) F. Beck and H. Gerisher, *Z. Elektrochem.* **63**, 500 (1959).

14) F. Lohmann, *Ber. Bunsenges. Physik. Chem.* **70**, 87 (1966).

15) R. F. G. Gardner, F. Sweet and D. W. Tanner, *J. Phys. Chem. Solid* **24**, 1175 (1963); *ibid.*, **1183** (1963). conductivity  $\delta$  is related with density  $n_e$ ,  $n_p$  and mobility  $\mu_e$ ,  $\mu_p$ , in the form  $\delta = n_e q \mu_e + n_p q \mu_p$ , where  $e$  and  $p$  represent electron and hole, respectively.  $\mu_e$  of  $\alpha\text{-Fe}_2\text{O}_3$  is a order of  $10^{-2} \text{ cm}^2 \text{ V}^{-1} \text{ sec}^{-1}$  and  $\mu_p$   $10^{-9} \text{ cm}^2 \text{ V}^{-1} \text{ sec}^{-1}$  for  $\alpha\text{-Fe}_2\text{O}_3$  containing 1 atom % Ti.

16) F. Beck and H. Gerisher, *Z. Elektrochem.* **63**, 943 (1959).

in Fig. 4. The current decreased slightly in the electrolyte containing  $\text{Ce}^{4+}$ . The mechanism of hole transfer is, therefore, doubtful. In addition, Fig. 1 shows that the current in the region B was the larger for the electrode with a smaller resistivity.

If it is assumed that the resistivity of  $\alpha\text{-Fe}_2\text{O}_3$  is almost completely determined by the electron density and its mobility,<sup>15)</sup> these results lead to the conclusion that the electron in the electrode is connected with the current in the region B. The situation in which the dissolution reaction of the  $\alpha\text{-Fe}_2\text{O}_3$  electrode proceeds by means of electron transfer is similar to the one observed in the dissolution reaction of heavily-doped N-type Ge.<sup>17)</sup> The nearly constant current observed in the region B conceivably appears as a result of the formation of a potential barrier in the electrode surface region or as a result of so-called "passivation" which occurs at the iron electrode in the potential comparable to the region B.<sup>18)</sup> The former mechanism is obeyed in the following hypothesis. The energy band of  $\alpha\text{-Fe}_2\text{O}_3$  will be bent upwards at the electrode in the potential comparable to the region B, since the flat-band potential of  $\alpha\text{-Fe}_2\text{O}_3$  is quite low as will be presented below. If the electron in the intermediate of the dissolution reaction must jump over this energy barrier in order to flow into the electrode during the process of the dissolution reaction, the current flow would naturally be hindered by this barrier,

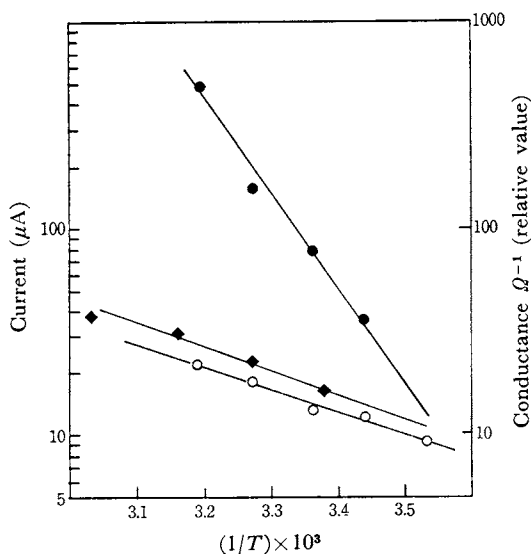


Fig. 5. Temperature dependence of electrode reactions and electrical transference in the electrode, electrode B

◆ conductance estimated from Pt- $\alpha\text{Fe}_2\text{O}_3$ -Pt system

● cathodic reaction at 0 V vs. SCE

○ anodic reaction at 0.7 V

17) R. Greth and M. E. Cowher, *J. Electrochem Soc.* **115**, 645 (1968).

18) K. Bohnhoffer, *Z. Metallkunde*, **44**, 77 (1953).

though its intermediate and its energy state are not clear at present. The finding that the activation energy of the reaction indicated by the current in the region B, 4.8 kcal/mol, was almost equal to that of the electrical transference of  $\alpha$ -Fe<sub>2</sub>O<sub>3</sub> estimated from the Pt- $\alpha$ -Fe<sub>2</sub>O<sub>3</sub>-Pt system, 5.0 kcal/mol, may support this mechanism.

The capacitance  $C$ -electrode potential  $V$  curves of the B electrode are shown in Fig. 6.  $C$  monotonously decreases with an increase in the electrode

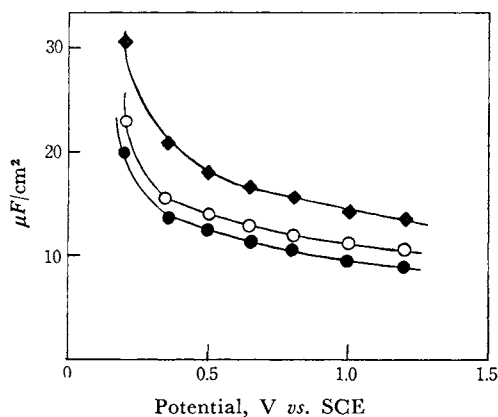


Fig. 6. Differential capacity of  $\alpha$ -Fe<sub>2</sub>O<sub>3</sub> containing Ti (1.0 atom%) in 0.1 N H<sub>2</sub>SO<sub>4</sub>. Contact material; Pt —◆— 2.5 kc —○— 5 kc —●— 10 kc

potential. The  $C$ - $V$  curves of the A, C and D electrodes are similar to that of the B.  $C$  was of an order of 10  $\mu$ F/cm<sup>2</sup>, as Fig. 6 shows. This is comparable to the double-layer capacity, as has often been pointed out,<sup>19,20</sup> and the measured  $C$  value normally refers to the space charge in the semiconductor surface region. Similarly, capacitance may be fixed in the passivation film when the passivated film exists on the electrode.<sup>21</sup> Therefore, if it is assumed that the measured  $C$  value refers to the space-charge capacity induced in the electrode surface, an abnormally large value of  $C$  may indicate that the estimation of the surface area was incorrect. Unfortunately, the correct estimation of the true surface area of the electrode of a sintered body is very difficult, especially on the oxide electrode. If the measured  $C$  value can be ascribed to the space-charge capacity in the electrode surface, then the flat-band potential can be estimated from the Mott-Schottky relation.<sup>19-21</sup> The discrepancies in the  $C$  values measured at various frequencies shown in

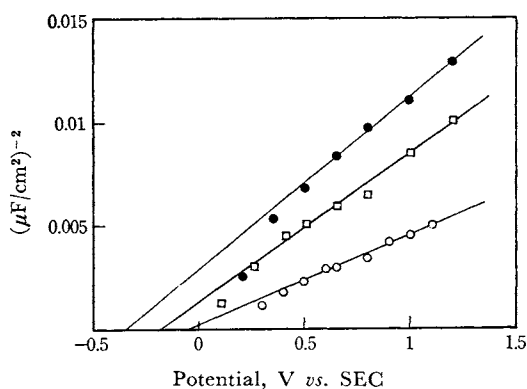


Fig. 7. Mott-Schottky plot for  $\alpha$ -Fe<sub>2</sub>O<sub>3</sub> electrode having platinum contact under exhaustion condition. electrode B —●— 0.1 N H<sub>2</sub>SO<sub>4</sub> —□— 0.5 N H<sub>2</sub>SO<sub>4</sub> —○— 1 N H<sub>2</sub>SO<sub>4</sub>

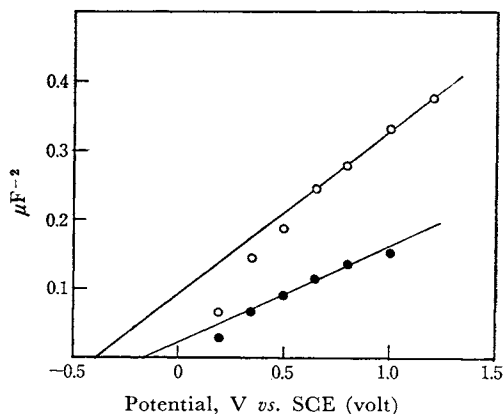


Fig. 8. Mott-Schottky plot for  $\alpha$ -Fe<sub>2</sub>O<sub>3</sub> electrode having indium contact under exhaustion condition. —○— 0.1 N H<sub>2</sub>SO<sub>4</sub> —●— 1 N H<sub>2</sub>SO<sub>4</sub>

Fig. 6 are due to the Faradic process or to the slow surface state on the electrode surface.<sup>22</sup> As the measured  $C$  values are more confused by these effects the lower the frequencies adopted,  $1/C^2$ - $V$  curves were obtained on the basis of the  $C$  value at 10 kc; they are shown in Figs. 7 and 8 for the A and B electrodes respectively. The finding that the  $1/C^2$ - $V$  curves show a linear relation above 0.5 V indicates that the space-charge layer was fixed in the electrode surface region above 0.5 V, since the  $C$  connected with the space-charge layer on the interface between  $\alpha$ -Fe<sub>2</sub>O<sub>3</sub> and the contact metal would be diminished with an increase in the electrode potential even if it did exist. The coincidence of the flat-band potential of the A electrode with that of the B indicates that a energy barrier on the interface between the contact metal and  $\alpha$ -Fe<sub>2</sub>O<sub>3</sub> did not have any serious effect on the  $C$ - $V$  curves, for the energy-barrier height which may be formed on

19) F. Dewald, *Bell System Tech. J.*, **39**, 615 (1960).

20) T. O. Rose and J. L. Wininger, *J. Electrochem. Soc.*, **113**, 184 (1966).

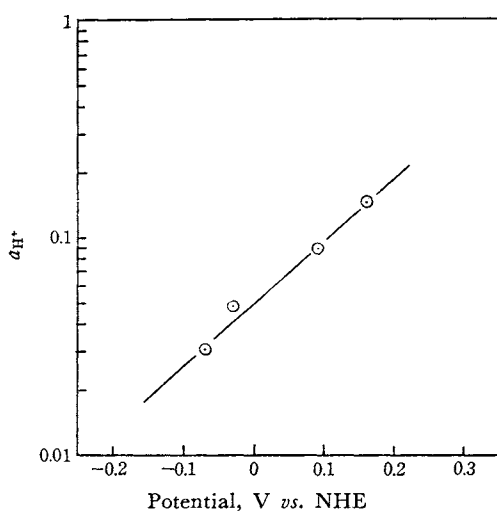
21) S. Toshima, *Denki Kagaku*, **34**, 565 (1966).

22) H. Gerisher, "Advance in Electrochemistry and Electrochemical Engineering," Vol. 1, ed. by P. Delahey and C. W. Tobias, Interscience Publishers, New York (1961), p. 163.

23) A. Kondo and Y. Takahashi, *Kogyo Kagaku Zasshi*, **71**, 1949 (1968).

TABLE 1. FLAT-BAND POTENTIAL FROM MOTT-SCHOTTKY PLOT

	Electrode		Flat-band potential V			
	atom% Ti	metal	0.1 N	0.2 N	0.5 N	1 N
A	1.0	In	-0.32	-0.24	-0.16	-0.16
B	1.0	Pt	-0.33	-0.24	-0.16	-0.13
				-0.22		-0.07
				-0.29		
				-0.31		
				-0.26		
C	0.6	Pt	-0.26			
D	0.6	Ag	-0.32			
F	0.4	Pt				
G	0.2	Pt				
Average ( <i>vs.</i> SCE)			-0.31	-0.275	-0.16	-0.10
After junction potential corrected (NHE)			-0.07	-0.03	+0.09	+0.16
$a_{H^+}$			0.032	0.0486	0.0895	0.146

Fig. 9. Flat-band potential of  $\alpha\text{-Fe}_2\text{O}_3$  electrode as a function of  $a_{H^+}$ .

the interface between Pt and  $\alpha\text{-Fe}_2\text{O}_3$  will be different from the one on the contact face between In and  $\alpha\text{-Fe}_2\text{O}_3$ . Pt has a larger work function, 5.10

eV,<sup>10)</sup> than In because In makes an ohmic contact with ZnO, which has the lower work function of 4.3 eV.<sup>23)</sup>

The estimated flat-band potentials in the electrolytes having different activities  $a_{H^+}$  of the proton are collected in Table 1. After the acid concentration of the electrolyte had been analytically determined and the liquid junction potential between the electrolyte and saturated KCl solution had been corrected according to Henderson's equation, the average values of the flat-band potential shown in Table 1 were plotted against  $a_{H^+}$ . They are presented in Fig. 9. The dependence of the flat-band potential on  $a_{H^+}$  may be attributed to the specific adsorption of the proton on the surface of the electrode, as has been observed at the lithiated NiO electrode.<sup>20)</sup> The flat-band potential,  $E$ , of the  $\alpha\text{-Fe}_2\text{O}_3$  electrode in the acid electrolyte was changed with  $a_{H^+}$  according to the following experimental equation estimated by the least-squares method,

$$E(\text{NHE}) = 0.45 + 0.35 \log a_{H^+}$$

The authors wish to thank Shinnichi Hamamatsu for preparing the electrode.